International journal of basic and applied research
www.pragatipublication.com
ISSN 2249-3352 (P) 2278-0505 (E)
Cosmos Impact Factor-5.86

Preparation and characterization of Hydroxyapatite Nanopowders by a simple sol-gel technique

Kannan Nithin K V
Associate Professor in Physics,
Kathir College of Engineering
Coimbatore,
Tamilnadu,
India.

Abstract
Hydroxyapatite (HA) nanopowders were prepared using simple sol–gel method with phosphoric pentoxide and calcium nitrate tetrahydrate. The effect of sintering temperatures on crystalline degree and composition of the HA phase, and also the effect of aging times on crystal size of the HA powder were studied using XRD, SEM, EDX and FTIR. At 700 and 800°C of sintering temperatures only HA phase was observed and the dominant phase of HA with small amounts of calcium oxide and β-Tricalcium Phosphate (β-TCP) were noticed at 800 and 900°C. In this method, less than100 nm HA powders were synthesized.

Keywords: EDX, FTIR, HA, Nanopowders, Sol–gel.

1. Introduction

In recent years, majority of the inorganic components for human bones, teeth and substitute material for hard tissues is made up of $Ca_{10}(PO_4)_6(OH)_2$ is known as HA is one of the calcium phosphate-based bioceramic material, has been extensively investigated for medical applications due to its excellent biocompatibility and tissue bio-activity properties [1–4]. A Due to this reason, researcher have been developed different methodologies of the preparation and processing of HA techniques like mechanochemical synthesis [5], combustion preparation [6], and various techniques of wet chemistry, such as direct precipitation from aqueous solutions [7], electrochemical deposition [8], sol–gel procedures [9], hydrothermal synthesis [10–12], an emulsion or micro-emulsion routes [13], gel-pyrolysis methods [14, 15] etc. At high temperature, solid-state synthesis of HA requires extensive mechanical mixing and lengthy heat treatment from oxide or inorganic salt powders [16, 17]. In most of the methods suffer from the complex and time-consuming procedures and sometimes mismatch in the solution behavior of the constituents. As a consequence, gross ceramics significant amount of impurity phases may be present. Sol-gel process offer advantages of good mixing of the starting materials and excellent chemical homogeneity [18–26]. In sol-gel method, pH value is low and also sintering temperature. In this process, calcium is mixed with phosphorus which is able to improving the chemical homogeneity. Many researchers have reported sol-gel processes [27–30] require a strict pH control and a long

Received: 5 April Revised: 13 April Accepted: 22 April
Index in Cosmos
May 2018 Volume 8 Number 5
UGC APPROVED

International journal of basic and applied research
www.pragatipublication.com
ISSN 2249-3352 (P) 2278-0505 (E)
Cosmos Impact Factor-5.86

time for hydrolysis. This method offers a simple sol-gel process that required no need to control pH value, vigorous stirring and a long time for hydrolysis.

2. Experimental

Nano size HA powders are produced using phosphorus pentoxide (P_2O_5) and calcium nitrate tetrahydrate ($Ca(NO_3)_2.4H_2O$) and are mixed with ethanol to form 0.5 mol and 1.67 mol solution respectively. The two solutions are mixed in a Ca/P molar ratio of 1.67 as an initial mixed precursor solution. At room temperature (27°C) the mixture is continuously stirred about 20 min, then heated in a water bath at 50°C for 2 h to get white transparent gel. The obtained gel is split into many parts and some parts are aged for 4 h at room temperature and then dried at 70°C for 36 h in an air oven. The dried gel are heated to 600, 700, 800, 900 °C in a muffle furnace, then cooled to room temperature without any external influence. The sintered products are smashed into powder with the help of granting instrument. Other parts are treated for different aging time (12 h, 24 h, 36 h, 48 h and 72 h) respectively. The obtained products are sintered at 700°C and 800°C to find the effect of aging time on formation and size of HA powders.
The prepared samples were characterized by X-ray diffratometer (XRD), Fourier transform infrared spectroscopy (FTIR), Elemental dispersive X-ray (EDX) analysis, Scanning electron microscopy (SEM).

3. Results and discussion

3.1. XRD analyses

The XRD pattern for a powder aged 4 h and sintered at 700°C is shown in Figure 1. Table 1 shows the d-spacing for HA are compared with the JCPDS [31] standard.

Received: 5 April Revised: 13 April Accepted: 22 April
Index in Cosmos
May 2018 Volume 8 Number 5
UGC APPROVED

International journal of basic and applied research
www.pragatipublication.com
ISSN 2249-3352 (P) 2278-0505 (E)
Cosmos Impact Factor-5.86

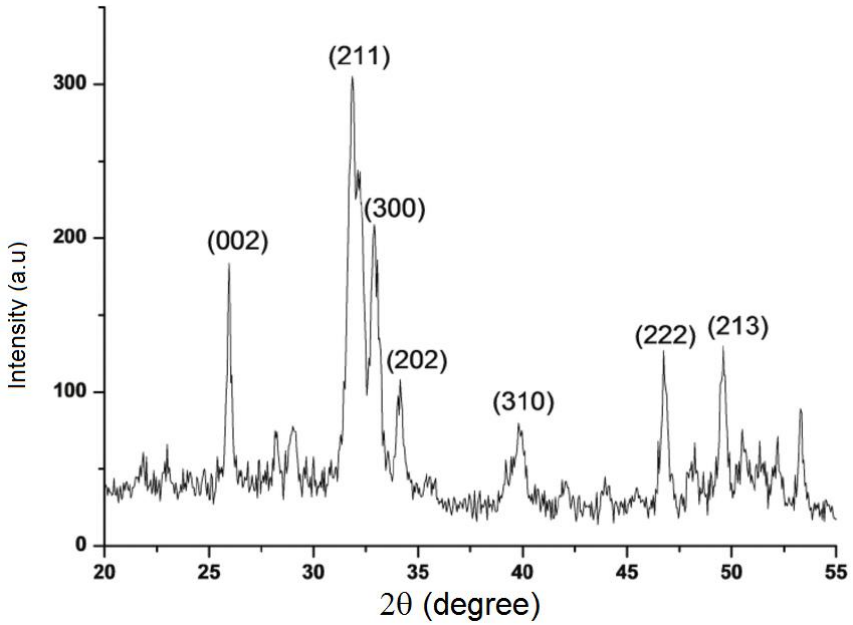

Fig. 1. X-ray diffraction pattern of HA powders. The powders were aged 4 h and sintered at 700°C.

Table 1 Plane spacing and intensities obtained from XRD

d (nm) experimental	JCPDS	Intensity experimental	JCPDS	(hkl)
0.3449	0.344	33	40	002
0.3075	0.308	14	18	210
0.2819	0.2814	100	100	211
0.2777	0.2778	48	60	112
0.2719	0.272	62	60	300
0.2634	0.2631	22	25	202
0.2292	0.2295	9	8	122
0.2262	0.2262	23	20	310
0.2149	0.2148	7	10	311
0.2060	0.2065	7	8	212
0.1947	0.1943	36	30	222
0.1893	0.189	17	16	213
0.1860	0.1841	41	40	312
0.1840	0.1806	19	20	004
0.1805	0.178	15	12	410

Received: 5 April Revised: 13 April Accepted: 22 April
Index in Cosmos
May 2018 Volume 8 Number 5
UGC APPROVED

International journal of basic and applied research
www.pragatipublication.com
ISSN 2249-3352 (P) 2278-0505 (E)
Cosmos Impact Factor-5.86

0.1779	0.1754	20	16	402
0.1757	0.1722	19	20	321
0.1720	0.1644	7	10	311
0.1643	0.1611	6	8	312
0.1616	0.1542	8	6	420

Experimental data from HA powder aged for 4 h and sintered at 700°C

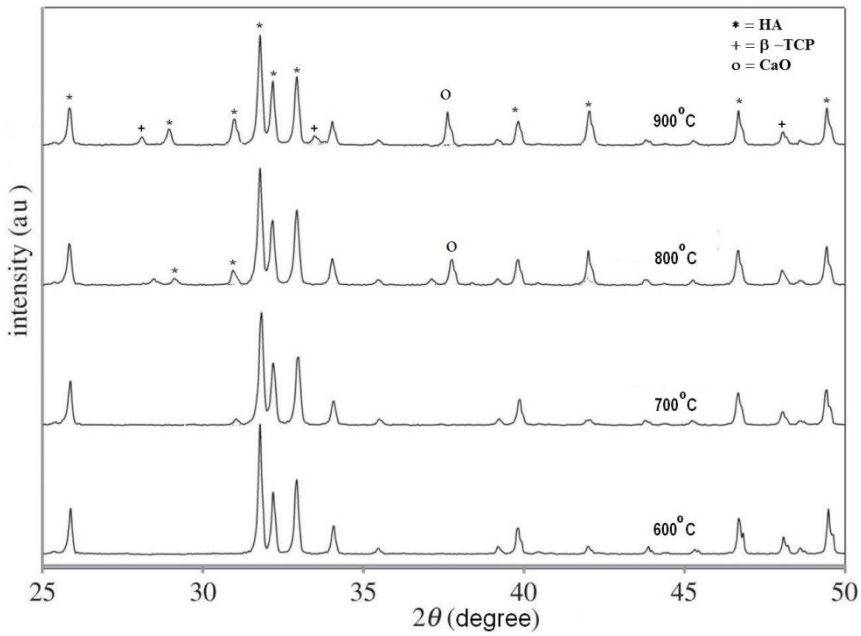

Fig. 2. XRD of HA powders for different sintering temperature.

From the result intensity and position of the lines have good competition with standard values. In addition from XRD pattern pure crystalline HA phase can be produced to the HA lines, no other line appears for the 700°C. The formation of HA are demonstrated in Figure 2 with different sintering temperature. It can be seen that the sintering temperature plays an important role in the formation of HA. While increasing the sintering temperature from 600 to 900°Cseveral of the HA lines become more distinct and also the widths of the lines become more narrow at higher temperatures, which suggests an increase in the crystallite degree. The additional crystalline phases (h-TCP and CaO) also appear at 800 and 900°C and no other crystalline phase presents besides HA at 600 and 700°C. It could be concluded that at high sintering temperature at 800°C or above the HA could be decomposed into h-TCP and CaO phases. For pure HA phase, the sintering temperature should be below 800°C

Received: 5 April Revised: 13 April Accepted: 22 April
Index in Cosmos
May 2018 Volume 8 Number 5
UGC APPROVED

International journal of basic and applied research
www.pragatipublication.com
ISSN 2249-3352 (P) 2278-0505 (E)
Cosmos Impact Factor-5.86

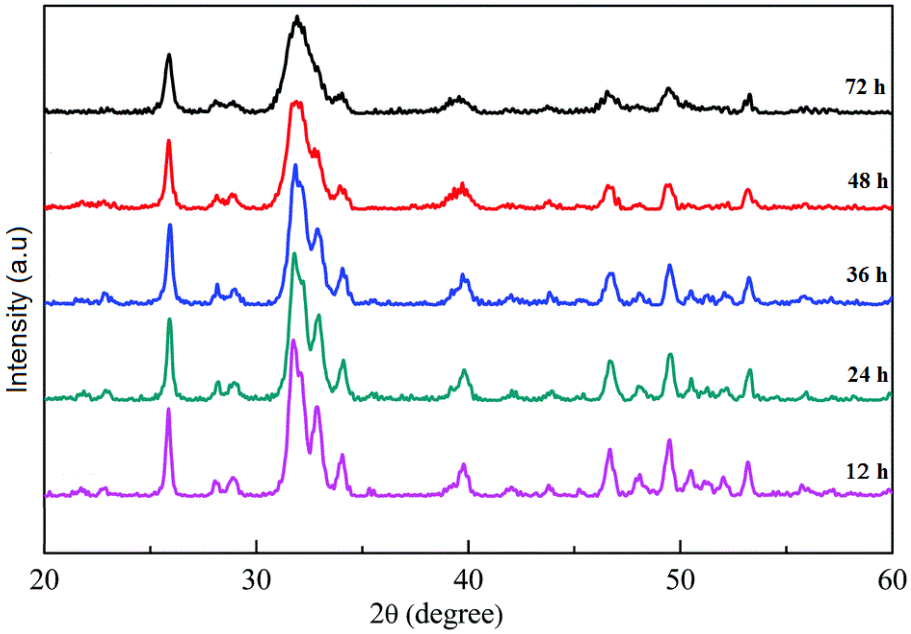

Figure. 3. XRD of HA powders for different aging times.

The XRD results for all samples with different aging times are shown in Figure 3. The samples are aged for 12 h, 24 h, 36 h, 48 h and 72 h and sintered at 700°C. The XRD results for all the samples sintered at 700°C are similar, that implies, no other phases present other than HA phase for different aging time. The XRD pattern demonstrates that the aging times has less effect on forming of pure HA phase than sintering temperature.

3.2. SEM analysis

Morphological study of hydroxyapatite was analyzed with scanning electron microscope (SEM). Figure 4 shows the SEM images of synthesised hydroxyapatite nanoparticles. The hydroxyapatite nanoparticles formed were highly agglomerated. The agglomeration of the nanoparticles might be because of Ostwald ripening. The spherical shaped particles with clumped distributions are visible from the SEM analysis. The SEM images show the spherical shaped morphology is predicated for the entire sample at 700°C sintering temperature [32].

Received: 5 April Revised: 13 April Accepted: 22 April
Index in Cosmos
May 2018 Volume 8 Number 5
UGC APPROVED

International journal of basic and applied research
www.pragatipublication.com
ISSN 2249-3352 (P) 2278-0505 (E)
Cosmos Impact Factor-5.86

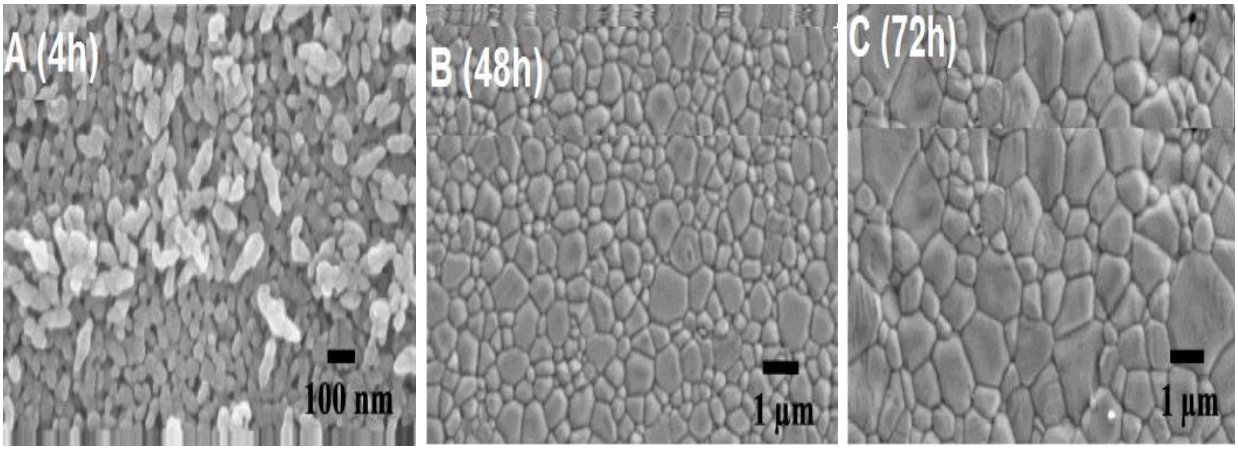

Figure 4. TEM images of HA powders sintered at 700°C. (a) Aged for 4 h, (b) aged for 48 h, (c) aged for 72 h.

However the size is increased due to the aging processes, for 4h aging time <100 nm sizes are predicated, where as for other aged samples size were increased to 300 nm for 48h and 3 µm for 72h (Figure 5). From the figure 3, the XRD peaks for 72 h aged sample are get broadening compare to the 4h aged samples and also the peak broadening get increasing while increasing the aging time. This implies that the particle size could be increased when aging time increased. It suggests that the sample synthesized for long aging time could contribute the growth and agglomerate.

3.3 FTIR analysis

Functional groups associated with hydroxyapatite samples with different temperatures were identified by FTIR spectroscopy. The FTIR spectra of the prepared samples are given in Figure 5. The HA spectra shows typical band coming from $PO4^{3-}$ with a maximum about 1022, 601 and 561 cm^{-1}. In addition at 3294 and 1666 cm^{-1} bands coming due to adsorbed water, at 2977 – 2848 cm^{-1} due to CO_2 coming from air are shown in figure 5B [33,34] and OH^- deformation band peak also appeared at 804 cm^{-1}. From FTIR spectra it is found that the width, intensity, and area of bands have explicit dependence on the particle size. As particle size increases, the intensity and area of IR bands usually decrease while the width of bands increases [35, 36].

Received: 5 April Revised: 13 April Accepted: 22 April
Index in Cosmos
May 2018 Volume 8 Number 5
UGC APPROVED

International journal of basic and applied research
www.pragatipublication.com
ISSN 2249-3352 (P) 2278-0505 (E)
Cosmos Impact Factor-5.86

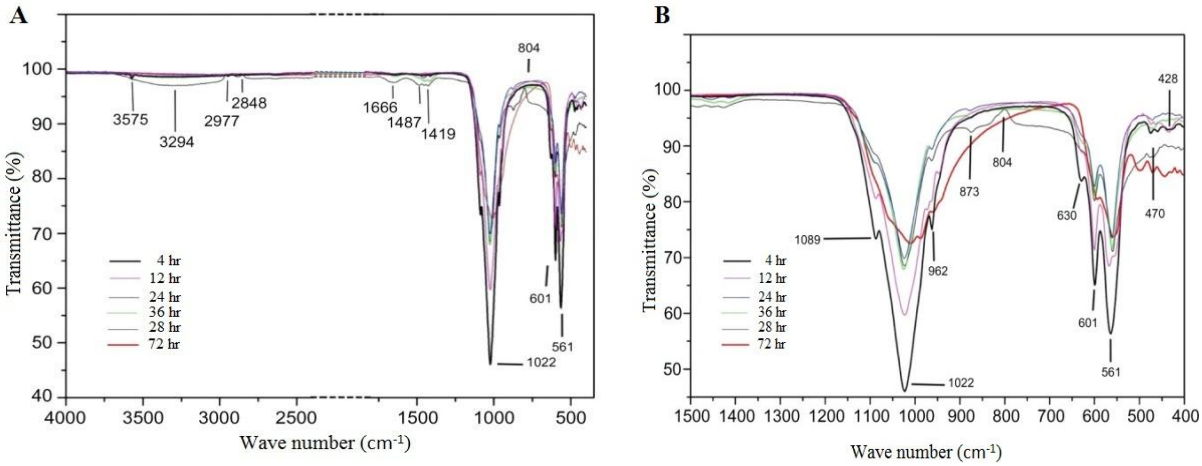

Figure 5. FTIR spectra of HA samples. Magnification in the wavenumber range 4000 to 400 cm-1 (**A**) and 1500 to 400 cm-1 (**B**).

3.3. EDX Analysis

The elemental analysis of the chemically produced HA powder is shown in Figure 6. The result represents the amount of calcium and phosphorus present in the sample. The weight and atomic percentage are also reported in the Figure 6. The EDX result shows the Ca/P ratio around 1.62 which is below 2 and acceptable. The ideal Ca/P ratio of HA is 1.67.

Table 2. Elemental composition of nano-hydroxyapitate.

Element	Weight (%)	Atomic (%)
OK	41.82	62.39
PK	21.36	15.57
CaK	36.82	22.04

Received: 5 April Revised: 13 April Accepted: 22 April
Index in Cosmos
May 2018 Volume 8 Number 5
UGC APPROVED

International journal of basic and applied research
www.pragatipublication.com
ISSN 2249-3352 (P) 2278-0505 (E)
Cosmos Impact Factor-5.86

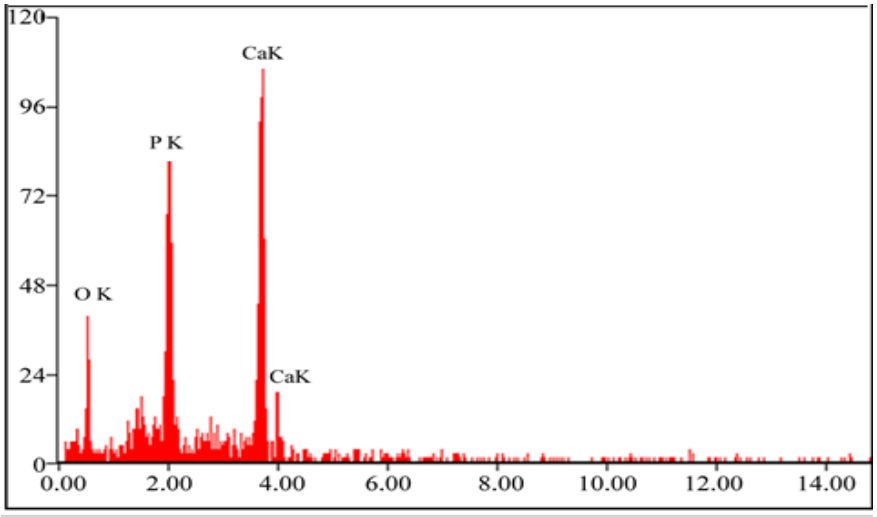

Figure 6. EDX spectrum of HA

4. Conclusion

Sol–gel method offers a simple method for synthesis of hydroxyapatite nanopowders. Sintering temperature and aging time implies the crystalline degree and morphology of the resulting nanopowders. By increasing the firing temperature, the crystalline degree of the HA nanopowders, and HA phase was observed at 700 and 800°C. The size of HA nanopowders sintered at 700°C and aged for 4 h is <100 nm. The XRD result reviles the crystallinity and the FTIR analysis evidences the phase purity of HA powder. From the EDX test of hydroxyapatite powder the ratio of Ca and P was found around 1.62.

References

[1] M. Vallet-Regi, J. Chem. Soc. Dalton Trans. 2 (2001) 97.
[2] L. Hermansson, L. Kraft, H. Engqvist, Adv. Ceram. Compos. Key Eng. Mater. 247 (2003) 437.
[3] T. Kokubo, H.-M. Kim, M. Kawashita, Biomater. 24 (2003) 2161.
[4] M. Shirkhanzadeh, J. Mater. Sci.: Mater. Med. 16 (2005) 37.
[5] W. Kim, Q.W. Zhang, F. Saito, J. Mater. Sci. 35 (2000) 5401.
[6] A.C. Tas, J. Eur. Ceram. Soc. 20 (2000) 2389.
[7] A. Lopez-Macipe, R. Rodriguez-Clemente, A. Hidalgo-Lopez, I. Arita, M.V. Garcia Garduno, E. Rivera, V.M. Castano, J. Mater.Synth. Process. 6 (1998) 121.
[8] L.Y. Huang, K.W. Xu, J. Lu, J. Mater. Sci., Mater. Med. 11 (2000)667.
[9] W.J. Weng, J.L. Baptista, Biomaterials 19 (1998) 125.
[10] M. Yoshimura, H. Suda, K. Okamoto, K. Ioku, J. Mater. Sci. 29 (1994) 3399.
[11] D. Janackovic, I. Jankovic, R. Petrovic, L. Kostic-Gvozdenovic, S. Milonjic, D. Uskokovic, Key Eng. Mater. 240–242 (2003) 437.

Received: 5 April Revised: 13 April Accepted: 22 April
Index in Cosmos
May 2018 Volume 8 Number 5
UGC APPROVED

International journal of basic and applied research
www.pragatipublication.com
ISSN 2249-3352 (P) 2278-0505 (E)
Cosmos Impact Factor-5.86

[12] J.B. Liu, X.Y. Ye, H. Wang, M.K. Zhu, B. Wang, H. Yan, Ceram. Int. 29 (2003) 629.
[13] G.K. Lim, J. Wang, S.C. Ng, L.M. Gan, J. Mater. Chem. 9 (1999)1635.
[14] A. Osaka, K. Tsuru, H. Iida, C. Ohtsuki, S. Hayakawa, Y. Miura, J. Sol–Gel Sci. Technol. 8 (1997) 655.
[15] H.K. Varma, S.S. Babu, Ceram. Int. 31 (2005) 109.
[16] G. De With, H.J.A. Van Dijk, N. Hattu, K. Prijs, J. Mater. Sci. 16 (1981) 1592.
[17] A. Bigi, S. Panzavolta, K. Rubini, Chem. Mater. 16 (2004) 3740.
[18] C.J. Brinker, G.W. Scherrer, Sol-Gel Science: The Physics and Chemistry of Sol-Gel Processing, Academic Press, San Diego, 1990.
[19] J. Livage, P. Barboux, F. Taulelle, J. Non-Cryst. Solids 147–148 (1992) 18.
[20] J. Zarzycki, J. Sol–Gel Sci. Technol. 8 (1997) 17.
[21] D.R. Uhlmann, G.J. Teowee, J. Sol–Gel Sci. Technol. 13 (1998) 153.
[22] C. Sanchez, F. Ribot, B. Lebeau, J. Mater. Chem. 9 (1999) 35.
[23] C. Sanchez, B. Lebeau, F. Ribot, M. In, J. Sol–Gel Sci. Technol. 19 (2000) 31.
[24] A. Baranauskas, D. Jasaitis, A. Kareiva, Vibr. Spectrosc. 28 (2002) 263.
[25] C. Sanchez, G.J.D.A.A. Soler-Illia, F. Ribot, D. Grosso, C.R. Chimie 6 (2003) 1131.
[26] B.L. Cushing, V.L. Kolesnichenko, C.J. O'Connor, Chem. Rev. 104 (2004) 3893.
[27] C.S. Chai, K.A. Gross, B. Ben-Nissan, Biomaterials 19 (1998) 2291.
[28] T.K. Anee, M. Ashok, M. Palanichamy, S. Naray-ana Kalkura, Mater. Chem. Phys. 80 (2003) 725.
[29] C.M. Lopatin, V. Pizziconi, T.L. Alford, T. Laursen, Thin Solid Films 326 (1998) 227.
[30] C.J. Brinker, G.W. Scherer, Sol–gel science, Academic Press, Boston, MA, 1990.
[31] JCPDS Card No. 9-432, 1994.
[32]Ferraz MP, Monteiro FJ, Manuel CM (2004). Hydroxyapatite nanoparticles: A review of preparation methodologies. J. Appl. Biomater. Biomech. 2:74-80.
[33]. T. Biro´ , I.J. Kova´cs, E. Kira´ly, G.y. Falus, D. Kara´tson, Z.s. Bendo,T. Fancsik, J.K. Sa´ndorne´. ''Concentration of Hydroxyl Defects in Quartz from Various Rhyolitic Ignimbrite Horizons: Results from Unpolarized Micro-FTIR Analyses on Unoriented Phenocryst Fragments''. Eur. J. Mineral. 2016. 28: 313–327.
[34]. J. Hlavay, K. Jonas, S. Elek, J. Inczedy. ''Characterization of the Particle Size and the Crystallinity of Certain Minerals by IR Spectrometry and Other Instrumental Methods - II. Investigations on Quartz and Feldspar''. Clays Clay Miner. 1978. 26: 139–143.
[35]. S.S. Palayangoda, Q.P. Nguyen. ''An ATR-FTIR Procedure for Quantitative Analysis of Mineral Constituents and Kerogen in Oil Shale''. Oil Shale. 2012. 29: 344–356.
[36] Beatrix Udvardi et al., effects of particle size on the attenuated total reflection spectrum of minerals, Applied Spectroscopy, 2016, 71(6),1157-1168.

Received: 5 April Revised: 13 April Accepted: 22 April
Index in Cosmos
May 2018 Volume 8 Number 5
UGC APPROVED